A Novel Active Filter for Mitigation of EMI and Other Adverse Effects of PWM Inverter-Fed AC Motor

Abdolreza Esmaeli[i]

ABSTRACT

This paper presents novel active filter for mitigation electromagnetic interference (EMI) and other adverse effects of pulse width modulation (PWM) inverter-fed AC motor system. An active filter proposed and devised for this system is characterized by sophisticated connection of two small separate filters, capable of mitigating all the adverse effects. This paper provides high frequency models of PWM inverter, rectifier, DC link, induction motor and long cable. The configuration and design procedure of the proposed filter is presented. The whole system is modeled and simulated by commercially available simulation software. A practical system with EMI measurement system have been suggested to test designed equipment ability in emitting EMI and other adverse effects to comply with electromagnetic compatibility (EMC) standards. The simulation results are verified by experimental results, which show the reduction characteristics of the shaft voltage, bearing current, common mode current, leakage current and EMI.

KEYWORDS

Electromagnetic compatibility, Electromagnetic Interference, Active filter, modeling, electrical machine, PWM inverter

1. INTRODUCTION

Conducted electromagnetic emissions currently produced by adjustable-speed AC drive systems are becoming the main interested subject for researchers and industry. Gary L. et al. reviews several main topics on electromagnetic interference (EMI) issues of modern pulse-width modulation (PWM) AC drives [1], and groups them into two aspects: conducted noise generation/propagation mechanism and drive system installation analysis. These are quite important guidelines to both manufactures and end users, although they are mainly based on realistic observations and expertise [2].

In addition to EMI, PWM AC drive systems have other adverse effects as common mode (CM) voltage [3], [4], [5] bearing current [6], [7], leakage current [8], shaft voltage [9] and over-voltage [10] in motor terminal. The current researchers up till now have only provided solutions for one or two isolated side effects and no collective solutions have yet been proposed [11], [12]. Simple filter model and induction motor model also presented in [13], [14]. A typical AC drive unit, which is commonly called an inverter, consists of a front-end line frequency AC-to-DC converter (rectifier), a DC bus with a capacitor filter and an output switch-mode DC-to-AC inverter, as shown in Figure 1. The rectifier together with the filter provides a filtered unregulated DC voltage on the DC bus. The solid-state devices of the DC-to-AC inverter are controlled under switch-mode in order to reduce the I^2R power loss. The output waveforms applied to the winding of the induction motor are square pulses with a modulated pulse-width (depending on the desired motor speed/voltage), which are different from the sinusoidal waveforms for which the AC motors were designed.

The size and cost of EMI filter components are important considerations in many power applications. One approach in reducing passive filter component size is the use of an active EMI filter. An active EMI filter replaces large passive components with smaller passives and some active control circuitry. Techniques exist to either reduce the amount of generating noise, or improve the performance of the passive filter.

This paper discusses the active technique mitigation of EMI and other adverse effects of PWM inverter AC drive system. PWM inverter fed AC motor drive system included motors, AC drive system (rectifier and PWM inverter system), leads, and other possible units that are used to develop one complete motor system to improve performances is constructed and tested with and without proposed active filter. The whole system is simulated by SABER simulator [15]. The simulation platform SABER is chosen because of the robust modeling engine, the ease of integrating mechanical components, and the large

i Dr. A. Esmaeli is with the Reactors and Accelerators Research and Development School, Nuclear Science & Technology Research Institute, P.O Box. 14155-1339, Tehran, Iran (e-mail: aesmaeli@aeoi.org.ir , esmaili20@yahoo.com).

library of existing models for a wide range of electrical components. SABER provides a good platform for device performance prediction in a system environment and also reliable data for EMI noise determinations.

This paper includes seven parts. First, introduction; second, modeling and filter design is the next. Part4 gives simulated results based on the presented models and the parameters of 4 kW induction motor system. Part 5 gives the experimental results and finally the conclusion and references are given in part 6 and 7 respectively.

2. MODELING

For an accurate high frequency (HF) model of AC motor drive systems, the HF parasitic current paths should take into account [16]. Figure 1 shows the Conventional adjustable speed drive system without EMI filter. HF models of different parts of Figure 1 presented in the following.

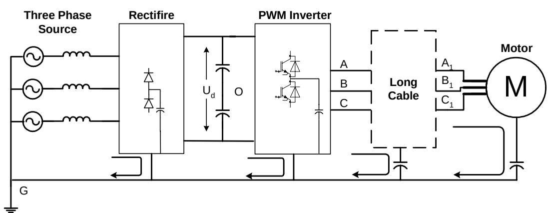

Figure 1: Conventional adjustable speed drive system

A. Rectifier and DC Link

The HF equivalent circuit of rectifier and DC link is shown in Figure 2. As an important role of parasitic capacitances between anode of diodes and ground in the HF current paths is considered in HF model of three-phase rectifier, C_{P1} is the parasitic capacitance of upper and C_{P2} is the parasitic capacitance of lower diodes in the rectifier shown in Figure 2. R_p and L_p are resistance and inductance parasitic value of DC capacitor of DC link.

B. Inverter

The three-phase inverter consisting of six IGBTs and six soft recovery diodes is used to drive the motor. The equivalent circuit of the three-phase voltage source inverter (VSI) is obtained by an extension of the switching cell. The inverter is composed of three legs, each of which consisting of two power IGBTs with parallel freewheeling diodes. The HF circuit model of the inverter system must take the main parasitic components of the inverter into account. Stray inductances of the connecting wires and parasitic capacitances between IGBT and heatsink are considered in the model. HF equivalent circuit of one leg of three-phase IGBT inverter is shown in Figure 3.

L_L is stray inductance of the connecting wires. C_P is stray capacitance of the collector and grounded heatsink. Between the collector and the heatsink, there appears a stray capacitance that affects principally leakage current generation. L_E and L_C are parasitic inductances of the emitter and collector of IGBT Model. Differential conducted emissions are affected by these inductances.

L_a is the a-phase line parasitic inductance and L_{L1} to L_{L4} are the line parasitic inductances from base and collector to PWM sources. Also the heatsink is modelled by one inductor (L_H) and one resistor (R_H). The value of the parasitic elements approached from RLC meter and devices datasheets for rectifier, DC link and inverter are presented in Table 1. All impedance measurements were performed with a resistance, inductance, and capacitance (RLC) meter with a measurement range of 75 kHz–30 MHz, following a proper calibration via a short-open procedure [17].

TABLE 1
THE HF PARAMETERS VALUE OF RECTIFIER, DC LINK AND INVERTER

C_{p1}	C_{p2}	R_p	L_p	C	L_L,L_E,L_C
75 pF	31 pF	2.1 Ω	25 nH	2.2 mF	3 nH
L_1,L_3	**L_2,L_4**	**L_a**	**L_H**	**R_H**	**C_P**
30 nH	50 nH	15 nH	125µH	8 Ω	220 pF

C. Induction Motor

A novel induction motor's model is shown in Figure 4. R, L and C are distributing parameters representing the HF coupling between the stator windings and rotor assembly.

Because of the partial insulation effect of the bearing grease and the electrical discharge machining (EDM) effect between the bearing balls and races, the motor bearings can be modeled as a capacitance C_b in parallel to a non-linear resistive circuit (R_L), and series with bearing ball and race contact resistance R_b. The bearing current, I_b, is flowing through the modeled wire impedance of measuring bearing current (L_w and R_w). C_g is the capacitance present across the stator and the motor laminations across the motor air gap. The coupling between the stator windings and the frame (stator) is considered as inductance (L_{sg}), resistance (R_{sg}) and capacitance (C_{sg}) since it mainly contributes to the total leakage current into the ground. Frame is modeled as resistance of R_g to ground. The values of HF parameters model of induction motor are presented in Table 2. By considering Figure1, the common mode voltage can be calculated by the following equation:

$$V_{CM} = \frac{V_{AG} + V_{BG} + V_{CG}}{3} = \frac{V_{AO} + V_{BO} + V_{CO}}{3} + V_{OG} = V'_{CM} + V_{OG} \quad (1)$$

where V_{AG}, V_{BG}, V_{CG}, V_{OG} represent the electric potential of point A, B, C, respectively, V_{AO}, V_{BO}, V_{CO} represent the voltage across A, B, C and O respectively.

To simplify the equation 1 can be written as (2) using switching function S_i (i=A, B, C), S_i=1 representing bottom switch being on.

$$V_{CM} = \frac{(S_A + S_B + S_C)U_d}{6} + V_{OG} = \begin{cases} \pm\dfrac{U_d}{2} + V_{OG} \\ \pm\dfrac{U_d}{6} + V_{OG} \end{cases} \tag{2}$$

where V_{OG} is the electric potential of point O.

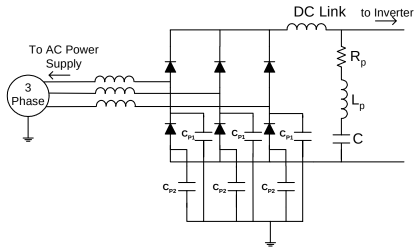

Figure 2. HF equivalent circuit of rectifier and DC link

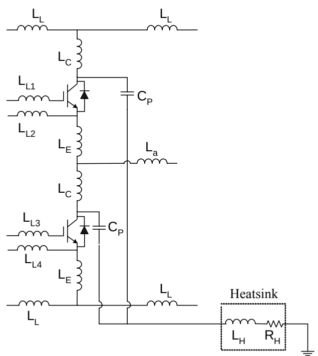

Figure 3. HF equivalent circuit of one leg of three-phase inverter

By considering the simplified model of induction motor shown in Figure 5 shaft voltage can be calculated by (3).

$$V_{sh} = V_{CM} \times \frac{Z_{rg}}{\frac{Z_{sr}}{3} + Z_{rg}} \tag{3}$$

where Z_{sr} is the impedance between the stator windings and rotor and impedance between the rotor and frame is Z_{rg} as defined in the following:

$$Z_{rg} = \frac{Z_g \times Z_b}{Z_g + Z_b} \quad , \; Z_{sr} = R + JL\omega + \frac{1}{JC\omega} \tag{4}$$

where Z_b and Z_g calculated as

$$Z_b = \frac{R_L \times \frac{1}{JC_b\omega}}{R_L + \frac{1}{JC_b\omega}} + R_b + R_W + JL_W\omega \tag{5}$$

$$Z_g = \frac{1}{JC_g\omega} \tag{6}$$

So the bearing current can be calculated by (7).

$$I_b = \frac{V_{sh}}{Z_b} \tag{7}$$

and leakage current can be developed as:

$$I_c = \frac{V_{CM}}{Z_{sg}/3} + \frac{V_{sh}}{Z_g} + \frac{V_{sh}}{Z_b} \tag{8}$$

where Z_{sg} is the impedance between the stator winding and ground.

$$Z_{sg} = R_{sg} + JL_{sg}\omega + \frac{1}{JC_{sg}\omega} \tag{9}$$

TABLE 2
THE HF PARAMETERS VALUE OF INDUCTION MOTOR

R_W	L_W	L	C	R	C_g
10 Ω	0.5µH	280 µH	18 pF	180 Ω	800 pF
R_L	R_b	C_b	R_{sg}	L_{sg}	C_{sg}
90KΩ	3 Ω	180pF	140 Ω	15 µH	800pF

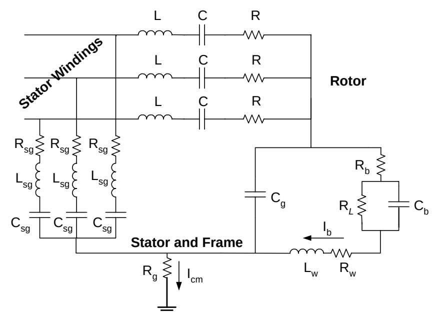

Figure 4. The HF model of induction motor

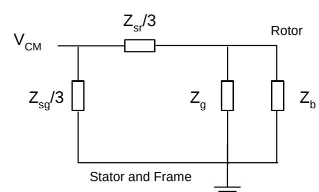

Figure 5. Simplified model of induction motor

D. *Long Cables*

The cable is modeled using the 20-stages π connection model as shown in Figure 6 [16]. The parameters of the cable model are therefore calculated by analyzing the behavior of the short-circuit impedance (Z_{sc}) and open-circuit impedance (Z_{oc}) over a broad range of frequency. The cable model series parameters (R and L) are associated to the behavior of the short-circuit impedance, while the parallel parameter (C) is associated to the behavior of the open-circuit impedances.

Equations (10), (11) and (13) are suggested to estimate the parameters of the cable model per-unit length, in which f_{low} and f_{high} are the lowest (100 Hz) and the highest (2 MHz) test frequencies respectively in the impedance measurements [16].

The values of the model's parameter are described per unit length (meter) in Table 3. For 20-stages of 100 meters cables, these values should multiply by 5.

$$R = \frac{2}{3} Real[Z_{sc}]_{f_{low}} \quad (10)$$

$$L = \frac{2}{3} \frac{1}{2\pi f_{high}} Image[Z_{sc}]_{f_{high}} \quad (11)$$

$$C = \left((2\pi f_{low}) \left(\frac{Real[Z_{oc}]_{f_{low}}}{Image[Z_{oc}]_{f_{low}}} \right) (2Real[Z_{oc}]_{f_{low}}) \left[\left(\frac{Image[Z_{oc}]_{f_{low}}}{Real[Z_{oc}]_{f_{low}}} \right)^2 + 1 \right] \right)^{-1} -$$
$$\left((2\pi f_{high}) \left(\frac{Real[Z_{oc}]_{f_{high}}}{Image[Z_{oc}]_{f_{high}}} \right) (2Real[Z_{oc}]_{fhigh}) \left[\left(\frac{Image[Z_{oc}]_{f_{high}}}{Real[Z_{oc}]_{f_{high}}} \right)^2 + 1 \right] \right)^{-1}$$
(12)

TABLE 3
HF PARAMETER VALUES OF LONG MOTOR CABLE

HF Parameter	Value
L	$2.8685 \times 10^{-7}\ H/m$
R	$0.0421\ \Omega/m$
C	$9.0867 \times 10^{-11}\ F/m$

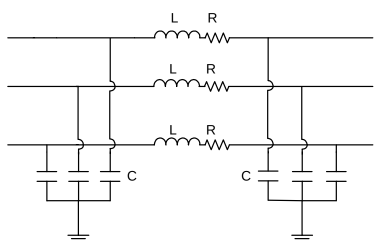

Figure 6. Twenty-stage serial-connected three-phase circuit of shield power cable model

As shown in Figure 1, motor terminal voltages with long cable can be described as the following:

$$V_{CM} = \frac{V_{A_1G} + V_{B_1G} + V_{C_1G}}{3} = \frac{V_{A_1O} + V_{B_1O} + V_{C_1O}}{3} + V_{OG} \quad (13)$$

As it is known, motor terminal voltages will approximately double approximately with long cable due to voltage reflection so common mode voltage can be described by (14) [18].

$$V_{CM} = \frac{V_{A_1O} + V_{B_1O} + V_{C_1O}}{3} + V_{OG} = \frac{2(V_{AO} + V_{BO} + V_{CO})}{3} + V_{OG} =$$
$$2V'_{CM} + V_{OG} = \begin{cases} \pm U_d + V_{OG} \\ \pm \dfrac{U_d}{3} + V_{OG} \end{cases} \quad (14)$$

By comparing (1) and (14), it is indicated that the common mode voltages at motor terminal with long cable also doubles. So it is very important to suppress common-mode voltage when long cable is used.

By simulation the AC motor drive systems with and without the proposed filter, the effect of proposed filter can be evaluated as discussed in the next sections.

3. Filter Design

The configuration of the proposed active filter with separate power supply is shown in Figure 7. The active common mode canceller (ACC) is composed of a push-pull type emitter follower circuit using two complementary transistors T_1 and T_2, a common-mode transformer, three impedances (Z_1) for common-mode voltage detection, and two DC voltage sources, three capacitors of C, inductor of L_3, and resistor of R.

In the previous ACC presented in [19], the inverter's DC supply V_d was used to power the active circuit (emitter follower) but here the emitter follower is powered from a separate source, unrelated to the inverter's power supply so the complementary transistors should not withstand voltages greater than V_d. However, since it is very difficult to find transistors rated for more than 400 V the proposed filter can solve this problem. The active filter can be used for induction motor rated 460 V or higher (like the present work where the DC voltage is over 400 volts) if the complementary transistors are powered from separated DC supplies (by value of $V_d/2n$) and use a CM transformer having a turns ratio of 1:n where n>1 as illustrated in Figure 2. The factor n is the ratio of the number of turns of any phase winding to the fourth winding (L_2). However, the exciting current of the CM transformer supplied from the ACC increases by a factor of n, and the rated current of the complementary transistors must be taken into account.

In this system, the output voltage of the emitter follower is superimposed on the inverter's output via the CM transformer (1:3). Hence, the CM voltage detection circuit composed of impedances Z_1 and Z_2 must have a dividing ratio of 1/3.

The main component of conducted EMI noise following the inverter is the CM current of motor from the CM voltage produced by the inverter, so it can be reduced greatly by reducing the CM voltage in motor terminal.

The EMI suppression can be implemented by an ACC, which is composed of push-pull type emitter follower circuit using transistors T_1 and T_2, a CM transformer and impedances Z_1 and Z_2 for CM voltage detection shown in Figure 7. The ACC is characterized by a sophisticated connection of a CM transformer, which can compensate CM voltage produced by inverter. To simplify the analysis of this circuit, the ACC is pre-digested as:

$$\begin{bmatrix} U_1(s) \\ U_2(s) \end{bmatrix} = \begin{bmatrix} L_1 s + 2Ms & \beta Ms \\ 3Ms & \beta L_2 s \end{bmatrix} \begin{bmatrix} I_1(s) \\ I_2(s) \end{bmatrix} \quad (15)$$

where $M = k\sqrt{L_1 L_2}$ and k is the coupling coefficient. Also β is the gain of transistors of emitter follower circuit. According to (15), the four winding transformer can be equivalent to a two winding transformer. The equivalent circuit of Figure 8(a) is shown in Figure 8(b), then the compensate scheme of ACC can be shown in Figure 9.

Figure 9 shows a CM equivalent circuit for the drive system. Here, V_{CM} means CM voltage produced by the inverter, and C_{CM}, L_{CM} and R_{CM} are stray capacitance, inductance and resistance components included in the CM circuit of the drive system, respectively.

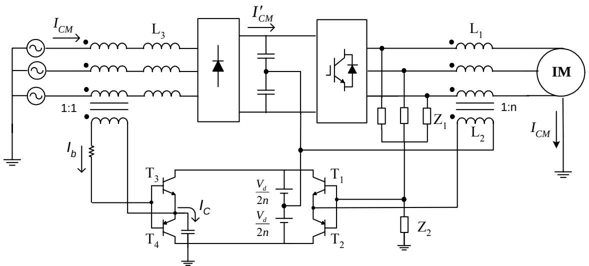

Figure 7. Configuration of conducted EMI filter for PWM inverter fed AC motor drive system

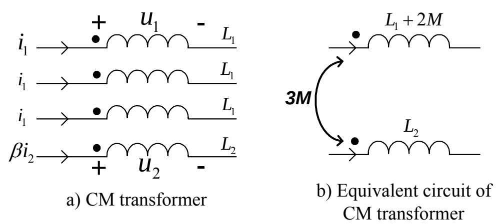

a) CM transformer

b) Equivalent circuit of CM transformer

Figure 8. CM transformer and its equivalent circuit

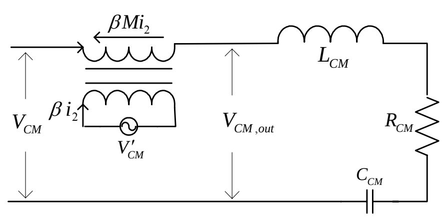

Figure 9. Compensate scheme diagram of ACC

The emitter follower circuit detects the CM voltage at the inverter output terminals, and produces the same voltage to the CM transformer. The transformer superimposes the CM voltage on the inverter outputs. As a result, the ACC can cancel the common-mode voltage generated by the inverter.

By considering Figure 7 and Figure 9 the following equations can be presented:

$$\begin{cases} V'_{CM} = \beta I_2(s) L_2 s \\ V_{CM} = \dfrac{Z_1(s)}{3} I_2(s) + V'_{CM} \\ V_{CM} = V_{CM,out} + \beta M s I_2(s) \end{cases} \tag{16}$$

Then the insertion loss effect *IL(s)* of ACC can be obtained from (16).

$$IL(s) = \frac{V_{CM,out}}{V_{CM}} = \frac{s\beta L_2 - \beta M s + Z_1(s)/3}{s\beta L_2 + Z_1(s)/3} \tag{17}$$

After eliminating CM voltage, the main source of the conducted EMI noise is CM current produced by the converter. The main work is how to reduce the conducted current from power source. Using another filter composed of inductor of L_3 at rectifier input, three Y-connected capacitors C_3 and a damping resistor R connected between the motor neutral point and rectifier input could complete the EMI reduction processing. This filter requires access to the ungrounded motor neutral point.

A. Design of the Filter Parameters

During the course of designing current compensate filter, proper parameters of transistor and CM transformer should carefully be selected, especially for the transistor. The transistor wide bandwidth, high voltage resistance, low loss and high gain are required in the filter. The impedance Z_1 and Z_2 in ACC should be composed of a resistor and a capacitor in series in order to avoid resonance. So (17) can be changed into (18).

$$IL(s) = \frac{3C_{Z1}(\beta L_2 - \beta M)s^2 + R_{Z1}C_{Z1}s + 1}{3\beta L_2 C_{Z1}s^2 + R_{Z1}C_{Z1}s + 1} \tag{18}$$

where R_{z1} and C_{z1} are resistance and capacitance of the impedance Z_1 respectively. In the process of CM voltage suppression, the insertion loss function *IL(s)* of ACC should have low-pass characteristics, so from (18):

$$\beta L_2 - \beta M = 0 \tag{19}$$

The relation between L_1 and L_2 should be limited by the following equation:

$$k = \sqrt{\frac{L_2}{L_1}} \tag{20}$$

Since the primary frequency of CM voltage produced by the inverter is focused on switching frequency and its multiples. So the resonance frequency of the CM voltage filter f_o should be much lower than the switching frequency f_s. The resonance frequency f_o is obtained from (18):

$$\omega_0 = 2\pi f_0 = \frac{1}{\sqrt{3\beta L_2 C_{z1}}} << 2\pi f_s \tag{21}$$

According to the experiment and experience, C_{z1}=180pf. The inductances and resistors can be calculated by the following Equations:

$$L_2 >> \frac{1}{3\beta C_{Z1}(2\pi f_s)^2} \tag{22}$$

$$L_1 = \frac{L_2}{k^2} \tag{23}$$

$$R_Z = 2\varsigma\sqrt{\frac{3\beta L_2}{C_{Z1}}} \tag{24}$$

where ς is the damping ratio.

4. SIMULATION RESULTS

SABER software was used for the simulation, which involved inserting the equivalent circuit of the presented models of this paper. The simulation results of the PWM inverter fed AC motor drive system when just ACC (Just one part of the proposed filter of Figure 7) is connected to the system are shown in Figure 10 and 12. Conducted EMI spectrum of PWM inverter fed AC motor drive system with the ACC is shown in Figure 10, which couldn't satisfy the EMI regulation. However conducted EMI just in low frequency is higher than the limit.

CISPR 22 regulation has been used globally for many years to determine compliance of electrical machine drive system with applicable limits as electromagnetic compatibility (EMC) regulation. Many economies like the European Union, Japan, Australia and New Zealand have adopted CISPR 22 into locally applicable standards. Other countries also accepted this regulation as international regulations. In this paper CISPR 22 regulations are considered. Limit of conducted emission of CISPR 22 (last version: 2004) for conducted emissions is 79 dBμV in the range of frequency 0.15-0.5 MHz and 73 dBμV in the range of frequency 0.5-30 MHz that is drawn in conducted EMI spectrum of simulations results (Figures 10 and 12). These limits are similar to other standards and regulations such as FCC class A limits (USA standards), EN 55022, IEC 61000 (European standards) and other acceptable standards.

Figure 11 shows shaft voltage (V_{sh}), bearing current (I_b) and CM current (I_{cm}) for PWM inverter fed AC motor drive system with the ACC.

As shown in Figure 11 peak value of shaft voltage by applying filter is reduced from 17 volts (without filter) to 4 volt. Also bearing current and CM current reduced to 3 mA and 1A (peak value) respectively, when they had higher value without ACC. CM current is reduced to ¼ of its value of without filter and bearing current is reduced to 1/10 of its original value by the ACC.

When the additional filter included L_3, R and C, connected between rectifier input and motor neutral point harmonic currents in the AC side of the PWM rectifier is eliminated. As discussed the effect of this additional loop in PWM inverter fed ac motor drive system to reduce CM current in the system, its effect in the new proposed filter shown in Figure 7, illustrated in Figure 12 and 13. Figure 12 shows conducted EMI spectrum of PWM inverter fed AC motor drive system with the proposed filter of Figure 7. The proposed EMI filter reduced conducted EMI to satisfy EMC regulations. As shown in Figure 12 conducted EMI of PWM inverter fed AC motor drive system connected to the proposed EMI filter met regulations. Comparison of Figure 10 and Figure 12 shows the effect of additional filter to the ACC to reduce conducted EMI.

Figure 8 shows shaft voltage (V_{sh}), bearing current (I_b) and CM current (I_{cm}) for PWM inverter fed AC motor drive system with the proposed filter (Figure 7). When the new proposed filter is connected, the shaft voltage, bearing and CM currents are suppressed almost perfectly as shown in Figure 13. As shown in Figure 13 shaft voltage reduced drastically and the peak value of the shaft voltages reach 50 mV at the maximum and also bearing current maximum value is several microamperes where these values cannot disturb system or be the cause of bearing damaging. CM current also is reduced, especially when we compare Figure 13 and Figure 11, the effects of additional filter can be shown.

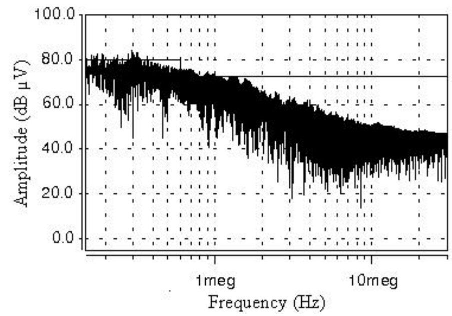

Figure 10. Conducted EMI spectrum of PWM inverter fed AC motor drive system with the ACC

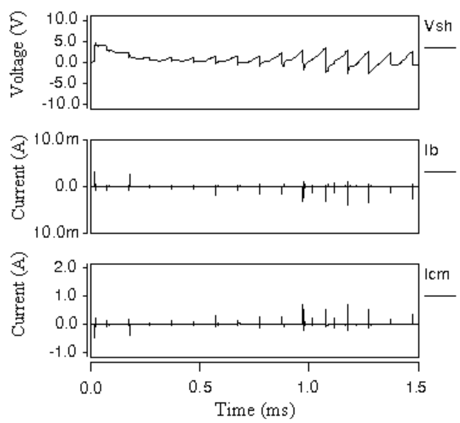

Figure 11. Shaft voltage, bearing current and CM current for PWM inverter fed AC motor drive system with the ACC

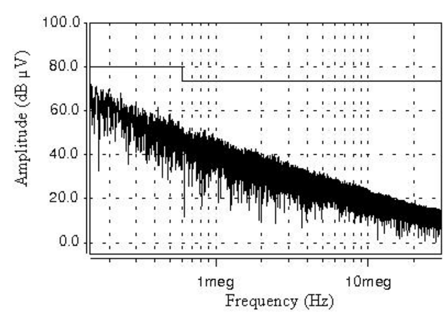

Figure 12. Conducted EMI spectrum of PWM inverter fed AC motor drive system with the proposed filter (Figure 2)

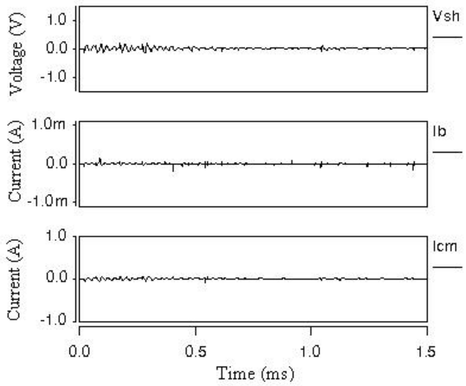

Figure 13. Shaft voltage, bearing current and CM current for the system of Figure 7

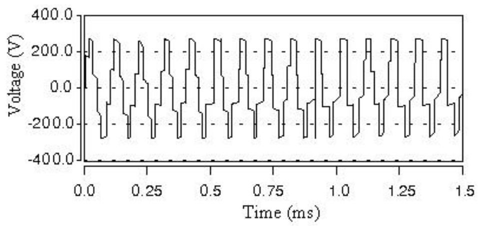

Figure 14. The voltage of the fourth winding (L2) of CM transformer (n=1) (When (n=3) the value will decrease to 1/3 of this value)

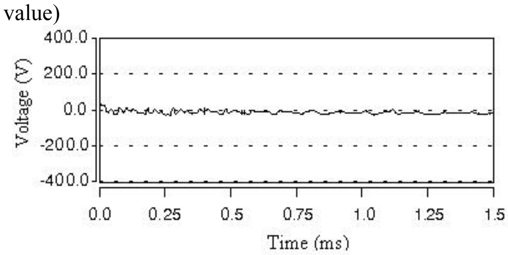

Figure 15. CM voltage in motor terminal when the proposed filter is connected to PWM inverter fed AC motor drive system

Since the results of the proposed filter is acceptable, it is not necessary to change the L_3 with a CM choke, although it will improve the circuit function but will cause of bulky circuit. To evaluate CM voltage reduction technique in the proposed filter, the voltage of the fourth winding (L_2) of CM transformer is shown in Figure 14. Ideally the waves of Figure 14 should be equal to CM voltage of inverter's output (in which case the turn ratio of n is equal to 1, but the parasitic value and loss in CM transformer, impedance (Z_1), transistors and other contributed systems make waveforms to be different and finally create CM voltage in motor terminals as it is shown in Figure 15.

However the CM voltage in motor terminal is almost eliminated. An alternative way to improve the ACC proposed in Figure 7 is the connection of another active filter in rectifier input to reduce the CM current in main side of PWM inverter fed AC motor drive system.

5. Experimental Results

The proposed conducted EMI filter shown in Figure 7 is connected to the PWM inverter AC motor drive system.

The test system as illustrated in Fig. 16, shows the 4 kW induction motor, 6 kW PWM inverter drive system, line impedance stabilization networks (LISN), EMI measurement system, proposed active filter and other measuring system for evaluating the adverse effects in the system. Standard regulations call for the utilization of LISN to be placed between AC power supply and the equipment under test (EUT) for measuring EMI.

This filter involves one ACC and one passive filter composed of three capacitors, one resistance and one inductor. After the proposed filter connected to the system, the results show that the adverse effects are reduced successfully. The results of elimination CM voltage and shaft voltage are presented in Figure 17. The measured CM voltage in motor terminals shows that the CM voltage is almost mitigated and the measured shaft voltage is eliminated. The main reason of the CM voltage reduction is the ACC employed between motor terminals and inverter output. The shaft voltage due to the CM voltage reduction and the connected passive filter between motor neutral point and rectifier input, shaft voltage is eliminated. Similarly bearing current and CM current are eliminated as shown in Figure 18.

The effect of active/passive filter on EMI is shown in Figure 19. The experimental results after employing the passive/active filter in the system have good agreement with the simulation results presented in simulation. Figures 17, 18 and 19 show that proposed filter could reduce all the adverse effects drastically. Especially this filter has better performance in reducing the CM voltage than single passive filter so it can reduce shaft voltage more than passive filter.

Considering the experimental results of both parts of proposed filter can be concluded that passive filter connected between motor neutral point and rectifier input has important role in reducing CM current.

Simulation and experimental results have good agreement as shown in Figure 12 and Figure 19 for EMI, and in Figures 13, 15, 17 and 18 for other adverse effects of PWM inverter.

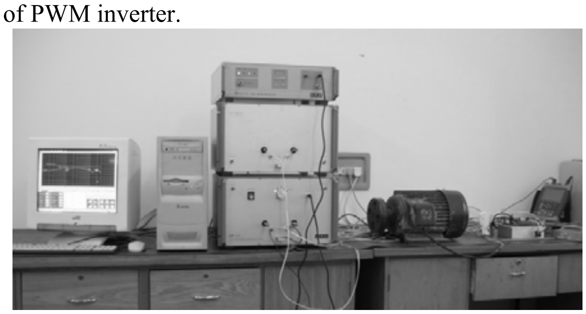

Figure 16. Experimental system to evaluate the adverse effects with filter

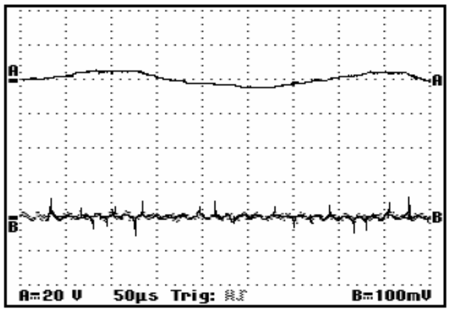

Figure 17. Measured CM voltage (A waveform) and shaft voltage (B waveform) (With active/passive EMI filter)

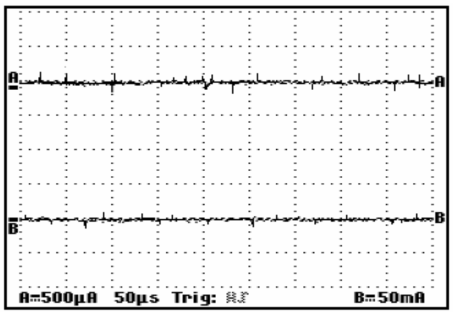

Figure 18. Measured bearing current (A waveform) and CM current (B waveform)(With active/passive EMI filter)

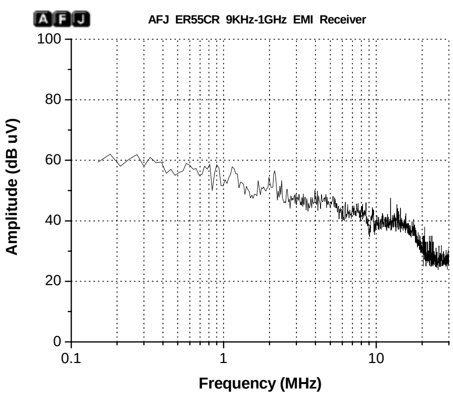

Figure 19. Conducted EMI (With active/passive EMI filter)

6. Conclusions

The theoretical analysis and comparisons based on simulation and experimental results of active method solution aimed at minimizing and eliminating the adverse effects of PWM inverters in AC motor drive systems has been presented in this paper. The proposed solution as an active filter's design procedure and analysis has been developed and has been verified by experimental results. An EMI elimination method based on two small passive and active filter connected between motor neutral point and rectifier input and also between inverter output and motor terminal has been proposed, designed, and tested for a 6 kW inverter fed 4 kW induction motor.

Experimental results have good agreement with simulation results that the proposed filter is effective and valuable in eliminating the adverse effects of PWM inverter in motor drive system. The proposed EMI filter reduced conducted EMI to satisfy EMC regulations (CISPR 22 regulation).

7. References

[1] G.L. Skibinski, R.J. Kerkman, and D. Schlegel, "EMI emissions of modern PWM AC drives. IEEE Industry Applications Magazine", vol. 5, no. 6, pp. 47-81, 1999.

[2] J. C. Crebier and J. P. Ferrieux, "PFC full bridge rectifiers EMI modeling and analysis-common mode disturbance reduction", IEEE Transactions on Power Electronics, vol. 19, no. 2, pp. 378 – 387, 2004.

[3] M.R. Baiju, K.K. Mohapatra and R.S. Kanchan, "A dual two-level inverter scheme with common mode voltage elimination for an induction motor drive", IEEE Transactions on Power Electronics, vol. 19, no. 3 pp. 794 – 805, 2004.

[4] S. Wei, N. Zargari, and B. Wu, "Comparison and mitigation of common mode voltage in power converter topologies", IEEE 39th Industry Applications conference, vol. 3, pp. 1852 – 1857, 2004.

[5] J. Adabi, F. Zare, G.F. Ledwich, A. Ghosh, "Leakage current and common mode voltage issues in modern AC drive systems", In proc. of Australasian Universities power engineering conference, pp. 641-646, 2007

[6] A. Muetze, and A. Binder, "Calculation of circulating bearing currents in machines of inverter-based drive systems", 39th IEEE Annual Meeting, Industry Applications Conference, vol. 2, pp. 720-726, 2004.

[7] D. Hyypio, "Mitigation of bearing electro-erosion of inverter-fed motors through passive common-mode voltage suppression", IEEE Transactions on Industry Applications, vol. 41, no. 2, pp. 576-583, 2005.

[8] C. Mei, J.C. Balda and W.P. Waite, "Minimization and cancellation of common-mode currents, shaft voltages and bearing currents for induction motor drives", IEEE 34th Annual Power Electronics Specialist Conference, vol. 3, pp. 1127-1132, 2003.

[9] R. Naik, T.A. Nondahl, and M.J, Melfi, "Circuit model for shaft voltage prediction in induction motors fed by PWM-based AC drives", IEEE Transactions on Industry Applications, vol. 39, no. 5, pp. 1294-1299, 2003.

[10] R. Naik, T.A. Nondahl, and M.J. Melfi, "Distributed parameter circuit model for shaft voltage prediction in induction motors fed by PWM based AC drives", 36th Annual Meeting Industry Applications Conference, vol. 2, pp. 1118-1122, 2001.

[11] Y. Lai, P. Chen, and H. Lee, "Optimal common-mode voltage reduction PWM technique for inverter control with consideration of the dead-time effects-part II applications to IM drives with diode front end", IEEE Transactions on Industry Applications", vol. 40, no. 6, pp. 1613-1620, 2004.

[12] R.S. Kanchan, P.N. Tekwani, and M.R. Baiju, "Three-level inverter configuration with common-mode voltage elimination for induction motor drive", IEE Proceedings-Electric Power Applications, vol. 152, no. 2, pp. 261-270, 2005.

[13] J. Drinovsky, J. Svacina, and Z. Raida, "Potential Worst-case System for Testing EMI Filters Tested on Simple Filter Models", Radio engineering, Vol. 17, No. 3, pp. 15-18, 2008.

[14] B. Mirafzal, G. Skibinski, and R. Tallam, "Determination of parameters in the universal induction motor model," IEEE Transactions on Industry Applications, vol.45, pp. 142 - 151, January /February 2009.

[15] SABER, Analogy, Inc., 9205 S.W. Gemini Drive, Beaverton, OR 97008, USA, release 5.1 edition.

[16] A. Esmaeli and L. Sun, "Modeling and simulation of induction motor drive system to investigate and mitigate of PWM inverter's adverse effects", Journal of Harbin Institute of Technology, vol. 14, No. 1, pp. 83-88, 2007.

[17] Agilent 4285A, Precision LCR Meter Data Sheet.

[18] X. Chen, D. Xu, F. Liu and J. Zhang, “A Novel Inverter-output passive filter for reducing both different and common dv/dt at the motor terminals in PWM drive system”, IEEE Transaction on Industrial electronics, vol. 54, pp. 419-426, 2007.

[19] C. Khun, V. Tarateeraseth, W. Khan-ngern, Masaaki Kando,” A simplified active Input EMI filter of common-mode voltage cancellation for induction motor drive” Proceedings of the ECTI International Conference (ECTI-CON 2007), pp. 93-96, 2007.